Journal of Physics: Conference Series **2889** (2024) 012006 doi:10.1088/1742-6596/2889/1/012006

Laser-cooling Cadmium Bosons and Fermions with Near Ultraviolet Triplet Excitations

Kurt Gibble

Department of Physics, The Pennsylvania State University, University Park, PA, 16802 USA

E-mail: kgibble@psu.edu

Abstract. Cadmium is laser-cooled and trapped with excitations to triplet states with UVA light, first using only the 67 kHz wide 326 nm intercombination line and subsequently, for large loading rates, the 25 MHz wide 361 nm $^3P_2 \rightarrow {}^3D_3$ transition. Eschewing the hard UV 229 nm $^1S_0 \rightarrow {}^1P_1$ transition, only small magnetic fields gradients, less than 6 G cm^{-1}, are required enabling a 100% transfer of atoms from the 361 nm trap to the 326 nm narrow-line trap. All 8 stable cadmium isotopes are straightforwardly trapped, including two nuclear-spin-$\frac{1}{2}$ fermions that require no additional repumping. We observe evidence of $^3P_2$ collisions limiting the number of trapped metastable atoms, report isotope shifts for ^{111}Cd and ^{113}Cd of the 326 nm $^1S_0 \rightarrow {}^3P_1$, 480 nm $^3P_1 \rightarrow {}^3S_1$, and 361 nm $^3P_2 \rightarrow {}^3D_3$ transitions, and measure the ^{114}Cd 5s5p $^3P_2 \rightarrow$ 5s5d $^3D_3$ transition frequency to be 830 096 573(15) MHz.

1. Introduction

Strontium, ytterbium and other atoms with two valence electrons are attractive for state-of-the-art quantum sensors such as optical-lattice atomic clocks and atom interferometers [1–8], for quantum gas experiments [9–14], and for quantum computation, information and simulation [15–20]. Yb, Ca, Cd and Hg have more than three stable spin 0 isotopes, enabling tests of fundamental physics through precise measurements of isotope shifts (ISs) [21–27]. The broad applicability of alkaline-earth-like atoms to high-coherence measurements is facilitated by their nearly forbidden clock and other intercombination transitions, from the singlet $^1S_0$ ground state to triplet $^3P_{J=0,1,2}$ states, as well as fast laser cooling, on the broad electric dipole allowed $^1S_0 \rightarrow {}^1P_1$ transition for most atoms (Ca, Sr, Yb, Mg, Cd and Zn). These atoms have clock transitions with mHz natural linewidths, their $^1S_0 \rightarrow {}^3P_1$ intercombination transitions have sub-MHz linewidths, which allow laser cooling to μK temperatures and lower, and their paired electron spins provide a natural insensitivity to perturbations from external magnetic fields. For the currently most accurate optical lattice clocks, based on Sr and Yb, one of the leading systematic errors is the frequency shift due to blackbody radiation (BBR) [1, 2, 4]. An attractive feature of Cd and Hg optical lattice clocks is their order of magnitude smaller sensitivities of their clock transitions to BBR than the Sr and Yb clock transitions [3, 4, 28, 29].

Previous laser cooling of Cd and Hg has used hard UV laser light, exciting the broad 91 MHz wide 229 nm $^1S_0 \rightarrow {}^1P_1$ Cd transition [28, 30, 31] and the 1.3 MHz wide 254 nm $^1S_0 \rightarrow {}^3P_1$ Hg intercombination transition [3, 4, 32]. These UVC sources are subject to degradation of non-linear crystals and optical coatings, making long-term operation, especially autonomous operation, challenging [3, 32]. Here, we demonstrate large loading rates and efficient laser-cooling of Cd

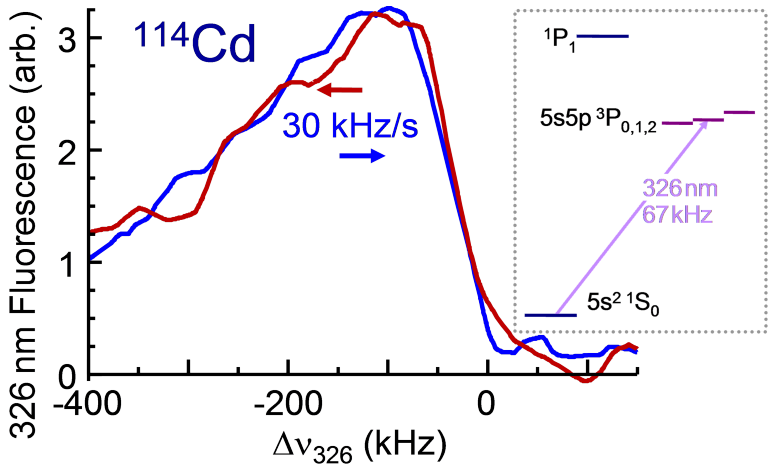

Figure 1. Fluorescence of a Cd MOT that uses only the 67 kHz wide $^1S_0 \rightarrow {}^3P_1$ 326 nm intercombination transition (see inset) to capture and trap atoms from an effusive source at 133 C. The blue (red) curve is the average of four frequency scans at $+(-)30\,\mathrm{kHz\,s^{-1}}$ and shows a sharp blue edge near the $^1S_0 \rightarrow {}^3P_1$ resonance.

using only near UV excitations to triplet states, with 326 nm and 361 nm light, in addition to two low-power blue optical pumping lasers, importantly, without having used 229 nm $^1S_0 \rightarrow {}^1P_1$ UVC light [30,31,33,34]. The multilevel lower state structure of the 361 nm broad-line magneto-optic trap (MOT) does not require the usual large magnetic field gradients of $^1S_0 \rightarrow {}^1P_1$ MOTs and provides polarization gradient cooling, facilitating a 100% transfer of atoms to the 326 nm narrow-line MOT.

We first demonstrate laser-cooling and trapping of approximately 10^4 Cd atoms from an effusive source using only the 67 kHz wide 326 nm $^1S_0 \rightarrow {}^3P_1$ intercombination transition [35,36] (see Fig. 1). While the narrow transition linewidth enables low Doppler cooling temperatures [28], in the absence of stimulated processes [37], the slow $^3P_1$ spontaneous emission limits the rate at which 326 nm photons can slow Cd atoms as they cross the laser beams. This is the narrowest transition used to capture atoms from a room-temperature (or hotter) source into an atom trap [38–40].

Next, we dramatically increase the laser-cooling capture rate using the dipole-allowed $^3P_2 \rightarrow {}^3D_3$ transition. For Cd, this transition is in the near UV, 361 nm in Fig. 2a), and has a reasonably broad 25 MHz linewidth. With other alkaline-earth atoms, this transition has been used in conjunction with the singlet transition to cool atoms to increase MOT and lattice loading fractions [41–43] and for high signal-to-noise detection [42]. Excitations from ^3P_J to other states, such as $^3P_0 \rightarrow {}^3D_1$, have been used to cool to sub-recoil temperatures [44, 45]; and $^3P_{0,1} \rightarrow {}^3S_1$, to increase the number of Sr atoms loaded into a magnetic trap, and subsequently an intercombination MOT [46]; and $^3P_1 \rightarrow {}^1D_2$ and $^3P_1 \rightarrow {}^1S_0$, to increase the scattering rate for a Ca intercombination MOT [47, 48].

Exciting the 361 nm UVA transition, we efficiently capture room temperature atoms and load a metastable $^3P_2 \rightarrow {}^3D_3$ MOT with all 6 of the stable nuclear-spin-zero Cd bosonic isotopes, ^{106}Cd to ^{116}Cd. We further show that no additional lasers are needed for hyperfine pumping to efficiently capture both nuclear-spin $I = \frac{1}{2}$ fermionic isotopes, ^{111}Cd and ^{113}Cd, in the metastable MOT. We observe evidence of $^3P_2$ collisional loss, report the ISs of three transitions, the 326 nm $^1S_0 \rightarrow {}^3P_1$, the 480 nm $^3P_1 \rightarrow {}^3S_1$ and the 361 nm $^3P_2 \rightarrow {}^3D_3$ transition, and measure the absolute frequency of the 361 nm $^3P_2 \rightarrow {}^3D_3$ transition, improving its previous uncertainty

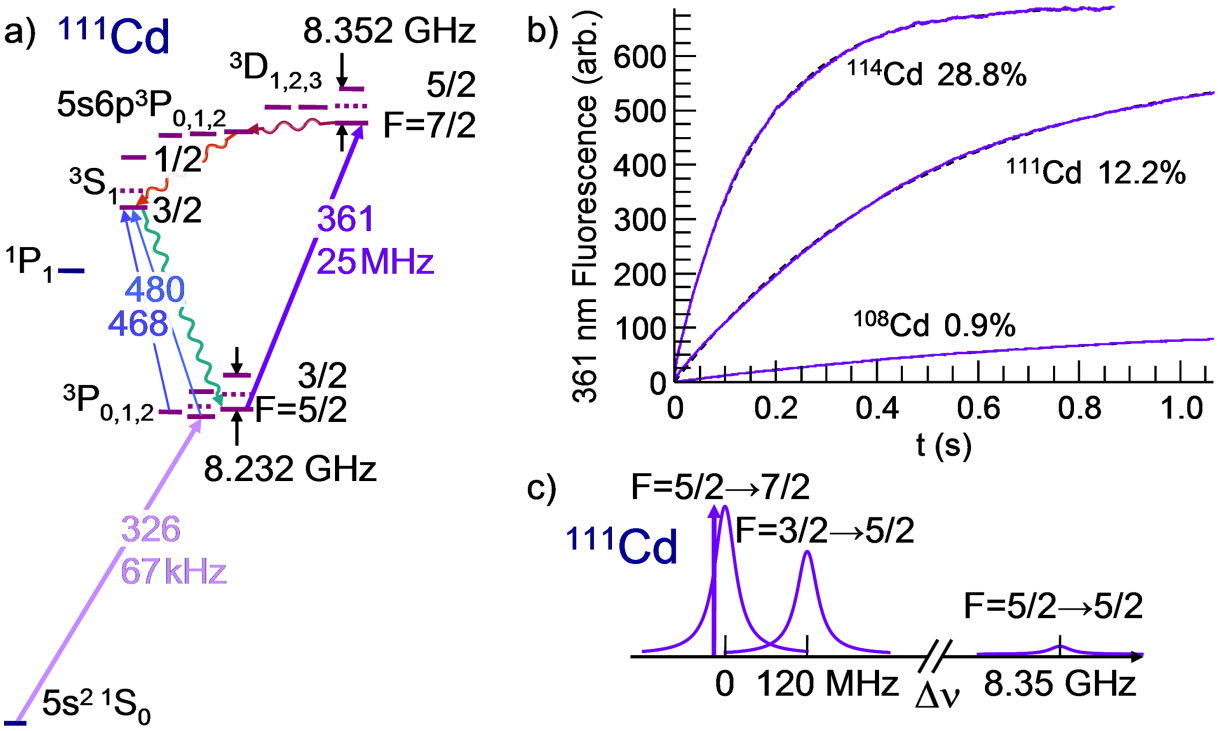

Figure 2. a) Energy levels of Cd fermions (solid) and bosons (dotted), where the annotated transition wavelengths are in nanometers. Atoms are excited to $^3P_1$ and optically pumped to $^3P_2$ via $^3S_1$ with 480 nm and 468 nm light. The 361 nm $^3P_2 \rightarrow {}^3D_3$ MOT transition is nearly closed, with a slow 11.4 μm and 1.4 μm cascade to 5s6p $^3P_2$ and $^3S_1$. The fermion hyperfine splittings from Table 1 are not depicted to scale and those of the $^1P_1$, $^3D_{1,2}$ and 5s6p $^3P_{1,2}$ states are omitted. b) Exciting the 25 MHz wide 361 nm $^3P_2 \rightarrow {}^3D_3$ transition efficiently captures the 8 Cd bosonic and fermionic isotopes. The faster saturation of the ^{114}Cd and ^{111}Cd loading than that for the 0.9% abundant ^{108}Cd suggests that $^3P_2$ collisional loss limits the number of atoms trapped. c) To trap ^{111}Cd and ^{113}Cd, the 361 nm laser is red-detuned from the $^3P_2$ $F = \frac{5}{2} \rightarrow {}^3D_3$ $F = \frac{7}{2}$ MOT transition. The inverted ^{111}Cd and ^{113}Cd fermion hyperfine structure and the larger hyperfine splitting of $^3D_3$ than that of $^3P_2$ in Table 1 enable convenient repumping (and cooling) of $^3P_2$ $F = \frac{3}{2}$ atoms via the $^3P_2$ $F = \frac{3}{2} \rightarrow {}^3D_3$ $F = \frac{5}{2}$ transition, from which the 361 nm laser is further red-detuned by 120 MHz for ^{111}Cd, and 125 MHz for ^{113}Cd.

by a factor of 20. This $^3P_2 \rightarrow {}^3D_3$ trapping may be applied to other alkaline-earth-like atoms, for example, Hg, where it can be challenging to maintain sufficient 254 nm power to capture many atoms in a $^1S_0 \rightarrow {}^3P_1$ MOT [3, 32].

Table 1. ^{111}Cd, and ^{113}Cd, hyperfine splittings of Fig. 2a) in MHz [35, 49–52].

A	$^3S_1$	$^3P_1$	$^3P_2$	$^3D_3$
111	−11626.2(13)	−6185.72(2)	−8232.341(2)	−8352.04(9)
113	−12162.9(14)	−6470.79(2)	−8611.586(4)	−8736.88(9)

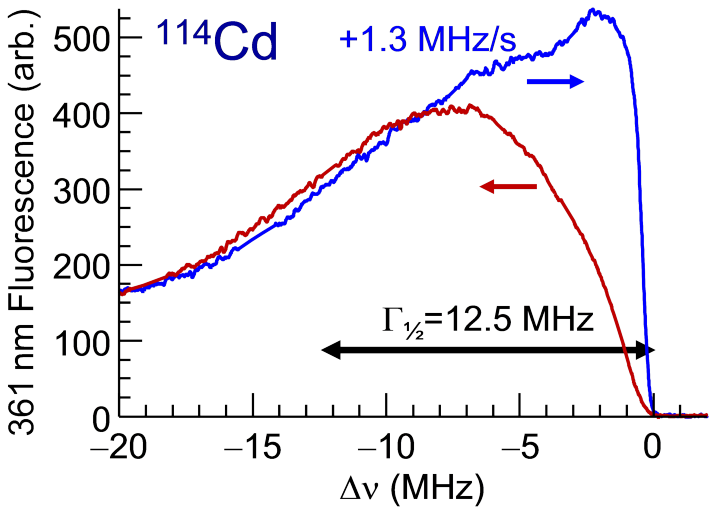

Figure 3. 361 nm metastable MOT fluorescence as the laser frequency is tuned across the $^3P_2 \rightarrow {}^3D_3$ resonance.

Table 2. Isotope shifts of Cd I fermions relative to ^{114}Cd, in MHz. We measure the 326 nm $^1S_0 \rightarrow {}^3P_1\ F = \frac{3}{2}$, the 361 nm $^3P_2\ F = \frac{5}{2} \rightarrow {}^3D_3\ F = \frac{7}{2}$ and the 480 nm $^3P_1\ F = \frac{3}{2} \rightarrow {}^3S_1\ F = \frac{3}{2}$ hyperfine transitions and calculate the transition centers-of-mass using the $^3P_1$, $^3P_2$, $^3S_1$ and $^3D_3$ hyperfine splittings in Table 1.

A	326 nm	361 nm	480 nm
111	861.6(10)	−227.4(10)	−334.2(11)
113	370.8(10)	−75.3(10)	−135.0(11)

2. Cadmium Intercombination and Metastable MOT's

2.1. Narrow-line 326 nm intercombination MOT

Trapping a detectable number of Cd atoms using only the 67 kHz wide 326 nm intercombination line in Fig. 1 is an important first step to bootstrap to the large loading rates of the 361 nm $^3P_2 \rightarrow {}^3D_3$ MOT. Our effusive source of Cd atoms with natural isotopic abundances has a 1.2 cm diameter, is 2.2 cm from the center of the MOT, and is heated to 120 C to 142 C. We begin with 50 to 150 mW of 326 nm light that is split into three retro-reflected beams with e^{-2} diameters of 8.5 mm to form a MOT with a quadrupole field gradient of 0.5 G cm^{-1} [53]. To increase the velocity capture range, an acousto-optic modulator (AOM) frequency modulates (FM) the 326 nm light at 50 kHz with a peak-to peak amplitude of 8.6 MHz [28]. We trap the six stable bosonic and fermionic isotopes, ^{110}Cd to ^{116}Cd, which have abundances greater than 7.5%. The number of trapped ^{114}Cd atoms versus frequency in Fig. 1 shows a sharp blue edge [54], which we use to measure isotope shifts [27]. The ^{111}Cd and ^{113}Cd fermions are trapped using their $^1S_0\ F = \frac{1}{2} \rightarrow {}^3P_1\ F = \frac{3}{2}$ hyperfine components and their ISs, given in Table 2, are consistent and more precise, as are the bosonic ISs [27], with other recent measurements [34]. To trap ^{106}Cd and ^{108}Cd, which have 1.25% and 0.89% abundances, we use the 361 nm $^3P_2 \rightarrow {}^3D_3$ MOT, described next, to increase the loading rate.

2.2. 361 nm Metastable MOT

With cold atoms trapped in the 326 nm intercombination MOT, it is straightforward to successively add and frequency tune the lasers for the 480 nm $^3P_1 \rightarrow {}^3S_1$ optical pumping, the 361 nm $^3P_2 \rightarrow {}^3D_3$ metastable MOT, and the 468 nm $^3P_0 \rightarrow {}^3S_1$ optical pumping [see Fig. 2a)]. The optical pumping to $^3P_2$ is well saturated with 100 μW of power in 12.6 mm diameter 468 nm and 8.7 mm diameter 480 nm laser beams. The 480 nm $^3P_1 \rightarrow {}^3S_1$ resonance can be easily found as this pumping extinguishes the 326 nm MOT fluorescence. We use 50 to 200 mW of 361 nm light that is intensity controlled and frequency shifted by an AOM before splitting into three retro-reflected MOT beams with e^{-2} diameters of 10.4 mm. The number of atoms depends weakly on the optimal MOT quadrupole gradient of 5.7 G cm^{-1}, notably smaller than the of order 200 G cm^{-1} gradients of $^1S_0 \rightarrow {}^1P_1$ singlet MOT's [28, 30, 31, 38]. Here, the 326 nm FM depth is larger, 16.3 MHz, consistent with the larger capture velocity of the 25 MHz wide 361 nm $^3P_2 \rightarrow {}^3D_3$ MOT [55]. From the saturation of the 361 nm fluorescence versus a pulsed intensity of the MOT beams, the number of trapped ^{114}Cd atoms is greater than 6×10^6. We trap all 6 spin 0 bosonic isotopes, which have no hyperfine structure [dashed levels in Fig. 2a)], including ^{106}Cd and ^{108}Cd with 1% abundances [Fig. 2b)]. As discussed below, the loading behavior in Fig. 3 for increasing frequency sweeps (blue curve), as well as the different loading time constants in Fig. 2b), suggests that $^3P_2$ collisional loss limits the number of trapped metastable atoms.

In addition to the 6 Cd bosonic isotopes, the 361 nm $^3P_2 \rightarrow {}^3D_3$ metastable MOT efficiently captures ^{111}Cd [Fig. 2b)] and ^{113}Cd nuclear-spin-$\frac{1}{2}$ fermions. Whereas additional repumping lasers are normally required for $J \rightarrow J+1$ MOT transitions with $J, I \neq 0$, especially for large nuclear spins [43, 46], no additional laser frequencies are required here for Cd. This is enabled by the negative nuclear magnetic moments of ^{111}Cd [Fig. 2a)] and ^{113}Cd and their $I = \frac{1}{2}$ nuclear spins. Each $J \neq 0$ state has only two hyperfine components, $F = J \pm I$, from the nuclear magnetic dipole interaction, with no electric quadrupole shifts for $I \leq \frac{1}{2}$. Table 1 gives the Cd hyperfine splittings and we highlight that the $^3D_3$ hyperfine splitting for ^{111}Cd(^{113}Cd) is 120(125) MHz larger than the $^3P_2$ hyperfine splitting [51, 52]. Combined with a negative nuclear magnetic moment, which yields the "inverted" ($^3S_1$, $^3P_1$,) $^3P_2$ and $^3D_3$ hyperfine structure, the $^3P_2\, F = \frac{3}{2} \rightarrow {}^3D_3\, F = \frac{5}{2}$ transition in Fig. 2c) is therefore 120 MHz blue detuned from the $^3P_2\, F = \frac{5}{2} \rightarrow {}^3D_3\, F = \frac{7}{2}$ metastable MOT cycling transition. As a result, atoms lost from the cycling transition to $^3P_2\, F = \frac{3}{2}$ are naturally repumped, cooled and trapped via the $^3P_2\, F = \frac{3}{2}, \rightarrow {}^3D_3\, F = \frac{5}{2}$ transition by the red detuned 361 nm MOT beams. The nuclear magnetic moment and resulting hyperfine splittings of ^{113}Cd in Table 1 are the same, within 5%, as for ^{111}Cd, allowing similarly large loading rates of ^{113}Cd as in Fig. 2b).

The low temperatures and small quadrupole magnetic field of the 361 nm metastable MOT facilitates an essentially complete transfer of captured atoms to the 326 nm intercombination MOT in Fig. 4. This compares to 20% to 30% direct transfer efficiencies from singlet to narrow-line Ca and Sr MOTs [47, 56]. Here, at $t = 0$, the 480 nm $^3P_1 \rightarrow {}^3S_1$ optical pumping light is extinguished. The 361 nm fluorescence decays in 0.7 ms as atoms no longer populate the $^3P_2$ state, e.g., through cascaded spontaneous emission from $^3D_3 \rightarrow 5s6p\,{}^3P_2 \rightarrow {}^3S_1 \rightarrow {}^3P_1 \rightarrow {}^1S_0$, and may then be captured by the FM-broadened 326 nm intercombination MOT. Resuming the 480 nm $^3P_1 \rightarrow {}^3S_1 \rightarrow {}^3P_2$ optical pumping with variable delays shows that 99.6(4)% of the atoms trapped in the metastable MOT are transferred to the intercombination MOT in Fig. 4b) and that it has a 1.2 s lifetime. Notably, this is significantly longer than the ≈ 0.5 s 361 nm MOT loading time in Fig. 4a) - if background gas collisions limited the lifetimes of both MOTs, the smaller trapping forces of the 326 nm MOT would normally yield a shorter lifetime.

Here, fine structure changing $^3P_2$ collisions, energy-pooling collisions or light-assisted collisions may shorten the loading time in Fig. 4a) and the number of atoms in Fig. 2b) in the 361 nm metastable MOT [57–59]. In Fig. 2b), the initial 361 nm MOT loading rates for ^{114}Cd, ^{111}Cd and ^{108}Cd are approximately proportional to their isotopic abundances while the

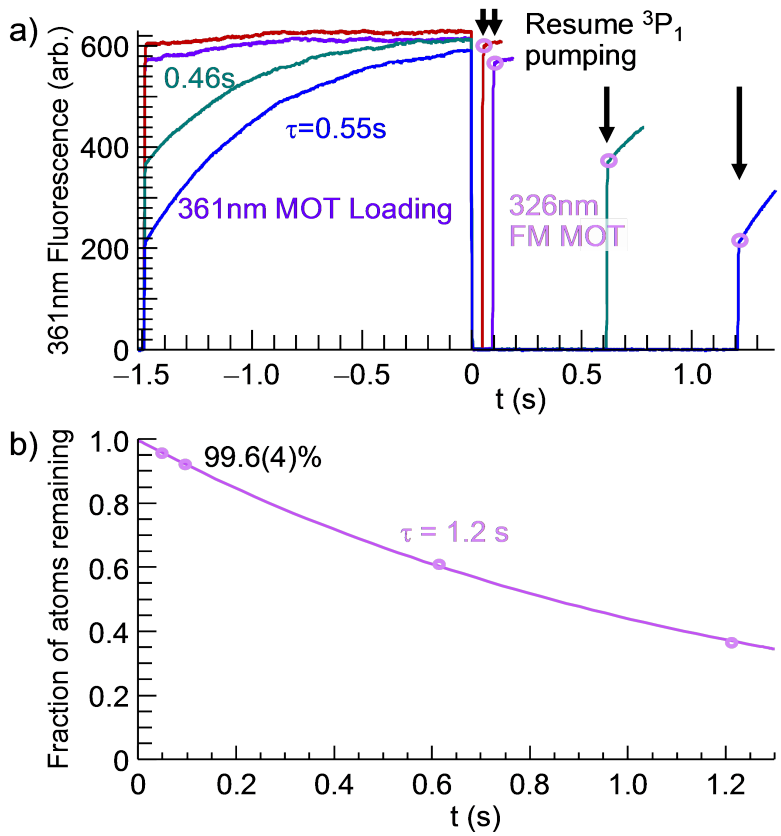

Figure 4. a) Inhibiting the 480 nm $^3P_1 \rightarrow {}^3S_1 \rightarrow {}^3P_2$ optical pumping in Fig. 2a) for a variable time transfers atoms from the metastable MOT to the the narrow-line MOT and back to the metastable MOT. b) A fit of the fraction of atoms remaining in the narrow-line MOT versus time shows 99.6(4)% of the atoms are captured and the lifetime is 1.2 s, well longer than the ≈ 0.5 s loading time of the metastable MOT. During the narrow-line MOT capture, the magnetic field gradient decreases from 5.7 G cm^{-1} to 0.6 G cm^{-1}.

asymptotic numbers of trapped atoms is limited more quickly for the abundant isotopes, in spite of a higher background Cd pressure for the ^{108}Cd data. Further supporting that $^3P_2$ collisions may limit the number of atoms trapped, the 361 nm fluorescence in Fig. 3 (blue curve) abruptly flattens as the metastable MOT light frequency increases beyond -7 MHz of resonance, and then the fluorescence suddenly increases at -3 MHz before falling rapidly to 0 at resonance. From images of the trap, the MOT becomes unstable with large atom numbers at these small detunings, as expected from repulsive radiation pressure forces [60]. Interestingly, here, this MOT instability appears to allow a larger number of trapped atoms with a lower density.

Figure 5 shows the 361 nm metastable MOT fluorescence when the 468 nm $^3P_1 \rightarrow {}^3S_1$ optical pumping light is extinguished for $\tau_e = 4$ ms to 14 ms. This transfers cold $^3P_2$ atoms to $^3P_0$, e.g., via decay from $^3D_3$ to 5s6p $^3P_2$ in Fig. 2a). These $^3P_0$ atoms are not trapped and begin to slowly leave the detection region, yielding less fluorescence just after they are repumped to $^3P_2$ at $t = 0$. Because the atoms are recaptured in much less than the MOT loading time, they do not exit the MOT laser beams volume during this time. After the 468 nm light is extinguished, the 326 nm excitation to $^3P_1$ and the 480 nm pumping from $^3P_1$ to $^3S_1$ to $^3P_2$, continues to load the 361 nm metastable MOT, albeit at a lower rate because some $^3P_1$ atoms excited to $^3S_1$ decay to $^3P_0$ instead of $^3P_2$. Nonetheless, for $\tau_e = 4$ ms, the 361 nm MOT fluorescence at $t = 4$ ms is

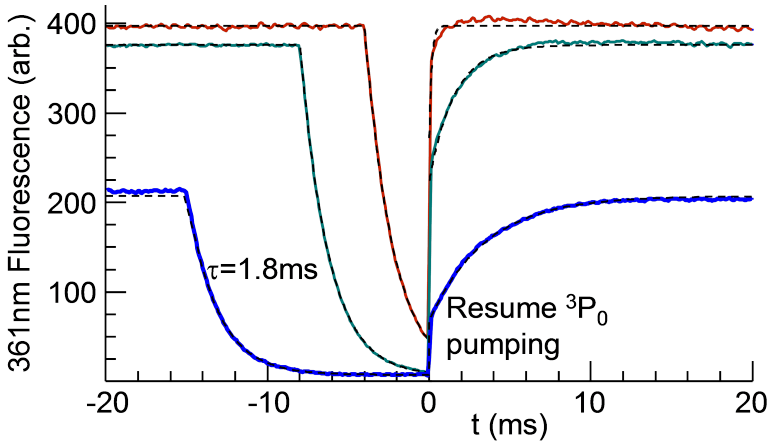

Figure 5. Atoms accumulate in the $^3P_0$ excited clock state with a time constant of 1.8 ms after the 468 nm $^3P_0 \rightarrow {}^3S_1$ optical pumping in Fig. 2a) is inhibited. The black dashed curves are exponential fits to the red, green and blue curves. For the red curve, after $^3P_0$ atoms are repumped to $^3P_2$, more atoms are detected at $t = 4$ ms than at $t = -4$ ms, when the optical pumping is turned off. This suggests that $^3P_2$ collisional loss limits the number of atoms in the metastable MOT. Here, the cycle repeats every 68 ms, which traps fewer atoms for the 14 ms $^3P_0$ holding time (blue curve).

greater than at $t = -4$ ms, consistent with a lower loss rate for atoms in $^3P_0$ than in $^3P_2$, and the dominant $^3P_2$ loss being fine structure changing collisions. For $\tau_e = 14$ ms in Fig. 5 (blue curve), the smaller number of trapped atoms is due to the short cycle time of 68 ms.

3. Laser System

To generate the four laser sources in Fig. 2a) [27, 61, 62], we begin with a 1083 nm extended-cavity diode laser (ECDL) that seeds a fiber amplifier, which is frequency doubled to 542 nm with LBO in a resonant cavity. We generate 361 nm UVA light for the metastable MOT with doubly resonant sum-frequency generation (SFG) of the 542 nm and 1083 nm light. The 326 nm UVA light for the intercombination MOT [27, 28, 61–63] is made in a second doubly resonant BBO cavity for SFG of the 542 nm light and 820 nm light from an ECDL and tapered amplifier. Finally, the low power blue 468 nm and 480 nm optical pumping light is generated with single-pass SFG of 1083 nm with 823 nm and 862 nm light in periodically-poled lithium niobate (PPLN) waveguides. The 1083 nm ECDL is frequency stabilised with a tunable offset to a ring reference-cavity, which is also used to monitor the 820 nm, 823 nm and 862 nm ECDL frequencies [27]. Saturated absorption of molecular I_2 provides an absolute frequency reference at 542 nm.

4. Isotope Shift and Absolute Frequency Measurements

We use the sharp blue-edge of the MOT fluorescence in Fig. 3 to measure the isotope shifts [27] and the absolute frequency of the $^3P_2 \rightarrow {}^3D_3$ transition. Relative to the the R(83)28-0 I_2 a_7 hyperfine component, the ^{114}Cd $^3P_2 \rightarrow {}^3D_3$ transition frequency is $\nu_{114} = \frac{3}{2}\nu_{R(83)28-0\,a_7} + 261(3)$ MHz, where a model of a number of I_2 absolute frequencies gives $\nu_{R(83)28-0\,a_7} = 553\ 397\ 541(10)$ MHz [64, 65]. This improves the previous uncertainty [66] by a factor of 20, yielding a 5s5d $^3D_3$ energy of 59 515.990 cm^{-1} for natural Cd, the value of [66], after a likely misprint is corrected [67]. The previous 300 MHz uncertainty contributed to some difficultly initially finding this broad transition - changing the frequency of our 361 nm light by more than the 10 MHz tuning range of the AOM requires changing the 820 nm laser

frequency and the dispersion of the 326 nm doubly-resonant SFG cavity to preserve the narrow-line MOT [61]. We use the blue MOT edge to measure the isotope shifts for the Cd bosons [27] and fermions, which are given in Table 2. We similarly report the 480 nm $^3P_1 \rightarrow {}^3S_1$ ISs from the optical pumping rate of the metastable MOT fluorescence, as in [27], which reported these ISs for Cd bosons.

5. Conclusions

Cadmium has a number of attractive properties for atomic clocks and interferometers and quantum gas experiments. These include narrow linewidth clock and other intercombination transitions, a small sensitivity of its clock transition to BBR, small sensitivities to external magnetic fields, a level structure that requires minimal repumping for laser cooling, and six bosonic isotopes and two nuclear-spin-$\frac{1}{2}$ fermionic isotopes. We demonstrate that all 8 Cd isotopes can be efficiently laser-cooled without exciting the hard UVC 229 nm $^1S_0 \rightarrow {}^1P_1$ transition. We begin by loading a MOT using only the Cd 67 kHz wide 326 nm $^1S_0 \rightarrow {}^3P_1$ UVA intercombination transition, the narrowest transition used to capture room temperature atoms. We dramatically increase the laser-cooling capture rate using the dipole-allowed 361 nm $^3P_2 \rightarrow {}^3D_3$ UVA transition to load a metastable MOT, with no additional repumping required for the Cd fermions.The $J = 2$ or $F = \frac{5}{2}$ substate structure of $^3P_2$ lower level of the metastable Cd MOT, along with the favorable $^3P_2 \rightarrow {}^3D_3$ hyperfine structure, yields the usual MOT behaviors of alkali atoms, in contrast to those of alkaline-earth singlet and intercombination MOTs. The $^3P_2 \rightarrow {}^3D_3$ metastable Cd MOT avoids cumbersomely large magnetic field gradients, provides low temperatures, and enables a 100% transfer of atoms to the narrow-line 326 nm MOT for subsequent cooling to microkelvin temperatures [28]. We observe evidence of collisional loss in the metastable MOT, report an absolute frequency of the $^3P_2 \rightarrow {}^3D_3$ transition, reducing its uncertainty by a factor of 20, as well as its isotope shifts and those of the 326 nm and 480 nm transitions [27] for the ^{111}Cd and ^{113}Cd fermions.

Capturing atoms with $^3P_2 \rightarrow {}^3D_3$ metastable MOTs may also efficiently collect atoms from an atomic beam that is optically pumped to $^3P_2$ and slowed with the $^3P_2 \rightarrow {}^3D_3$ transition, or a beam slowed by low-power $^1S_0 \rightarrow {}^1P_1$ light, avoiding the $^1S_0 \rightarrow {}^1P_1$ MOT and its required large magnetic field gradients [38–40]. Beyond Cd, these techniques may be particularly useful for Hg [3, 32], requiring only low power UVC light, as well as for Sr [43] and Yb, and possibly Zn [68], Ca and Mg [42]. Avoiding UVC light, or reducing its required power, is advantageous for long-term operation of future Zn, Cd and Hg clocks and other quantum sensors, particularly in remote environments.

Acknowledgments

We gratefully acknowledge stimulating and helpful conversations with U. Sterr, S. Gupta, A. Yamaguchi, H. Katori, A. Kramida, and E. Tiemmann and contributions of D. Schussheim [61, 62].This material is based upon work supported by the U.S. National Science Foundation under award No. 2012117.

References

[1] Ludlow A D, Boyd M M, Ye J, Peik E and Schmidt P O 2015 *Rev. Mod. Phys.* **87**(2) 637–701 https://link.aps.org/doi/10.1103/RevModPhys.87.637
[2] Beloy K *et al* 2021 *Nature* **591** 564–569 ISSN 1476-4687 https://doi.org/10.1038/s41586-021-03253-4
[3] McFerran J J, Yi L, Mejri S, Di Manno S, Zhang W, Guéna J, Le Coq Y and Bize S 2012 *Phys. Rev. Lett.* **108**(18) 183004 https://link.aps.org/doi/10.1103/PhysRevLett.108.183004
[4] Ohmae N, Bregolin F, Nemitz N and Katori H 2020 *Opt. Express* **28** 15112–15121 http://www.opticsexpress.org/abstract.cfm?URI=oe-28-10-15112
[5] Tarallo M G, Mazzoni T, Poli N, Sutyrin D V, Zhang X and Tino G M 2014 *Phys. Rev. Lett.* **113**(2) 023005 https://link.aps.org/doi/10.1103/PhysRevLett.113.023005

[6] Abe M *et al* 2021 *Quantum Science and Technology* **6** 044003 https://dx.doi.org/10.1088/2058-9565/abf719
[7] Tino G M 2021 *Quantum Science and Technology* **6** 024014 https://dx.doi.org/10.1088/2058-9565/abd83e
[8] Bandarupally S, Tinsley J N, Chiarotti M and Poli N 2023 *Journal of Physics B: Atomic, Molecular and Optical Physics* **56** 185301 https://dx.doi.org/10.1088/1361-6455/acf3bf
[9] Takasu Y, Maki K, Komori K, Takano T, Honda K, Kumakura M, Yabuzaki T and Takahashi Y 2003 *Phys. Rev. Lett.* **91**(4) 040404 https://link.aps.org/doi/10.1103/PhysRevLett.91.040404
[10] Kraft S, Vogt F, Appel O, Riehle F and Sterr U 2009 *Phys. Rev. Lett.* **103**(13) 130401 https://link.aps.org/doi/10.1103/PhysRevLett.103.130401
[11] Stellmer S, Tey M K, Huang B, Grimm R and Schreck F 2009 *Phys. Rev. Lett.* **103**(20) 200401 https://link.aps.org/doi/10.1103/PhysRevLett.103.200401
[12] de Escobar Y N M, Mickelson P G, Yan M, DeSalvo B J, Nagel S B and Killian T C 2009 *Phys. Rev. Lett.* **103**(20) 200402 https://link.aps.org/doi/10.1103/PhysRevLett.103.200402
[13] Cazalilla M A and Rey A M 2014 *Reports on Progress in Physics* **77** 124401 https://dx.doi.org/10.1088/0034-4885/77/12/124401
[14] Chen C C, González Escudero R, Minář J, Pasquiou B, Bennetts S and Schreck F 2022 *Nature* **606** 683–687 ISSN 1476-4687 https://www.nature.com/articles/s41586-022-04731-z
[15] Gorshkov A V, Hermele M, Gurarie V, Xu C, Julienne P S, Ye J, Zoller P, Demler E, Lukin M D and Rey A M 2010 *Nature Physics* **6** 289–295 ISSN 1745-2481 https://doi.org/10.1038/nphys1535
[16] Daley A J 2011 *Quantum Information Processing* **10** 865 ISSN 1573-1332 https://doi.org/10.1007/s11128-011-0293-3
[17] Pagano G, Scazza F and Foss-Feig M 2019 *Advanced Quantum Technologies* **2** 1800067 https://onlinelibrary.wiley.com/doi/abs/10.1002/qute.201800067
[18] Madjarov I S, Covey J P, Shaw A L, Choi J, Kale A, Cooper A, Pichler H, Schkolnik V, Williams J R and Endres M 2020 *Nature Physics* **16** 857–861 ISSN 1745-2481 https://doi.org/10.1038/s41567-020-0903-z
[19] Bloch I, Dalibard J and Nascimbène S 2012 *Nat. Phys.* **8** 267–276 ISSN 1745-2481 https://doi.org/10.1038/nphys2259
[20] Schäfer F, Fukuhara T, Sugawa S, Takasu Y and Takahashi Y 2020 *Nature Reviews Physics* **2** 411–425 ISSN 2522-5820 https://doi.org/10.1038/s42254-020-0195-3
[21] Counts I, Hur J, Aude Craik D P L, Jeon H, Leung C, Berengut J C, Geddes A, Kawasaki A, Jhe W and Vuletić V 2020 *Phys. Rev. Lett.* **125**(12) 123002 https://link.aps.org/doi/10.1103/PhysRevLett.125.123002
[22] Ono K, Saito Y, Ishiyama T, Higomoto T, Takano T, Takasu Y, Yamamoto Y, Tanaka M and Takahashi Y 2022 *Phys. Rev. X* **12**(2) 021033 https://link.aps.org/doi/10.1103/PhysRevX.12.021033
[23] Figueroa N L, Berengut J C, Dzuba V A, Flambaum V V, Budker D and Antypas D 2022 *Phys. Rev. Lett.* **128**(7) 073001 https://link.aps.org/doi/10.1103/PhysRevLett.128.073001
[24] Hur J *et al* 2022 *Phys. Rev. Lett.* **128**(16) 163201 https://link.aps.org/doi/10.1103/PhysRevLett.128.163201
[25] Solaro C, Meyer S, Fisher K, Berengut J C, Fuchs E and Drewsen M 2020 *Phys. Rev. Lett.* **125**(12) 123003 https://link.aps.org/doi/10.1103/PhysRevLett.125.123003
[26] Zheng X, Dolde J, Lochab V, Merriman B N, Li H and Kolkowitz S 2022 *Nature* **602** 425–430 https://doi.org/10.1038/s41467-023-40629-8
[27] Ohayon B, Hofsäss S, Padilla-Castillo J E, Wright S C, Meijer G, Truppe S, Gibble K and Sahoo B K 2022 *New Journal of Physics* **24** 123040 https://dx.doi.org/10.1088/1367-2630/acacbb
[28] Yamaguchi A, Safronova M S, Gibble K and Katori H 2019 *Phys. Rev. Lett.* **123**(11) 113201 https://link.aps.org/doi/10.1103/PhysRevLett.123.113201
[29] Dzuba V A and Derevianko A 2019 *Journal of Physics B: Atomic, Molecular and Optical Physics* **52** 215005 https://dx.doi.org/10.1088/1361-6455/ab4434
[30] Brickman K A, Chang M S, Acton M, Chew A, Matsukevich D, Haljan P C, Bagnato V S and Monroe C 2007 *Phys. Rev. A* **76**(4) 043411 https://link.aps.org/doi/10.1103/PhysRevA.76.043411
[31] Kaneda Y, Yarborough J M, Merzlyak Y, Yamaguchi A, Hayashida K, Ohmae N and Katori H 2016 *Opt. Lett.* **41** 705–708 https://opg.optica.org/ol/abstract.cfm?URI=ol-41-4-705
[32] Lavigne Q, Groh T and Stellmer S 2022 *Phys. Rev. A* **105**(3) 033106 https://link.aps.org/doi/10.1103/PhysRevA.105.033106
[33] Tinsley J N, Bandarupally S, Penttinen J P, Manzoor S, Ranta S, Salvi L, Guina M and Poli N 2021 *Opt. Express* **29** 25462–25476 https://opg.optica.org/oe/abstract.cfm?URI=oe-29-16-25462
[34] Hofsäss S, Padilla-Castillo J E, Wright S C, Kray S, Thomas R, Sartakov B G, Ohayon B, Meijer G and Truppe S 2023 *Phys. Rev. Res.* **5**(1) 013043 https://link.aps.org/doi/10.1103/PhysRevResearch.5.013043
[35] Lurio A and Novick R 1964 *Phys. Rev.* **134**(3A) A608–A614 https://link.aps.org/doi/10.1103/PhysRev.134.A608
[36] Czajkowski M, Bobkowski R and Krause L 1989 *Phys. Rev. A* **40**(8) 4338–4343 , this more recent measurement suggests a 3.0(1) μs lifetime and a 53(2) kHz linewidth https://link.aps.org/doi/10.1103/PhysRevA.40.4338

[37] Norcia M A, Cline J R K, Bartolotta J P, Holland M J and Thompson J K 2018 *New Journal of Physics* **20** 023021 https://dx.doi.org/10.1088/1367-2630/aaa950
[38] Kawasaki A, Braverman B, Yu Q and Vuletic V 2015 *Journal of Physics B: Atomic, Molecular and Optical Physics* **48** 155302 , report capturing Yb using only its 184 kHz 556 nm intercombination transition. https://dx.doi.org/10.1088/0953-4075/48/15/155302
[39] Kuwamoto T, Honda K, Takahashi Y and Yabuzaki T 1999 *Phys. Rev. A* **60**(2) R745–R748 https://link.aps.org/doi/10.1103/PhysRevA.60.R745
[40] Lee J, Lee J H, Noh J and Mun J 2015 *Phys. Rev. A* **91**(5) 053405 https://link.aps.org/doi/10.1103/PhysRevA.91.053405
[41] Grünert J and Hemmerich A 2002 *Phys. Rev. A* **65**(4) 041401 https://link.aps.org/doi/10.1103/PhysRevA.65.041401
[42] Friebe J *et al* 2011 *New Journal of Physics* **13** 125010 https://dx.doi.org/10.1088/1367-2630/13/12/125010
[43] Akatsuka T, Hashiguchi K, Takahashi T, Ohmae N, Takamoto M and Katori H 2021 *Phys. Rev. A* **103**(2) 023331 https://link.aps.org/doi/10.1103/PhysRevA.103.023331
[44] Zhang X, Beloy K, Hassan Y S, McGrew W F, Chen C C, Siegel J L, Grogan T and Ludlow A D 2022 *Phys. Rev. Lett.* **129**(11) 113202 https://link.aps.org/doi/10.1103/PhysRevLett.129.113202
[45] Chen C C, Siegel J L, Hunt B D, Grogan T, Hassan Y S, Beloy K, Gibble K, Brown R C and Ludlow A D 2024 *Phys. Rev. Lett.* **133**(5) 053401 https://link.aps.org/doi/10.1103/PhysRevLett.133.053401
[46] Barker D S, Reschovsky B J, Pisenti N C and Campbell G K 2015 *Phys. Rev. A* **92**(4) 043418 https://link.aps.org/doi/10.1103/PhysRevA.92.043418
[47] Curtis E A, Oates C W and Hollberg L 2001 *Phys. Rev. A* **64**(3) 031403 https://link.aps.org/doi/10.1103/PhysRevA.64.031403
[48] Sterr U, Degenhardt C, Stoehr H, Lisdat C, Schnatz H, Helmcke J, Riehle F, Wilpers G, Oates C and Hollberg L 2004 *Comptes Rendus Physique* **5** 845–855 ISSN 1631-0705 fundamental metrology https://www.sciencedirect.com/science/article/pii/S1631070504001525
[49] Frömmgen N *et al* 2015 *The European Physical Journal D* **69** 164 ISSN 1434-6079 https://doi.org/10.1140/epjd/e2015-60219-0
[50] Brimicombe M S W M, Stacey D N, Stacey V, Hühnermann H, Menzel N and Bleaney B 1976 *Proceedings of the Royal Society of London. A. Mathematical and Physical Sciences* **352** 141–152 https://royalsocietypublishing.org/doi/abs/10.1098/rspa.1976.0168
[51] Faust W, McDermott M and Lichten W 1960 *Phys. Rev.* **120**(2) 469–469 https://link.aps.org/doi/10.1103/PhysRev.120.469
[52] Chantepie, M and Lecluse, Y 1971 *J. Phys. France* **32** 415–419 https://doi.org/10.1051/jphys:01971003205-6041500
[53] The MOT is loaded for 400 ms and the atom fluorescence is integrated for 16.67 ms after the laser's FM is inhibited and its intensity and detuning are ramped [62]. A subsequent background, also integrated for 16.67 ms after the atoms are cleared with a blue laser detuning, is subtracted. The direction of the MOT magnetic field gradient is then reversed and its background, from two more integrations, is additionally subtracted, giving an updated number of trapped atoms every 907 ms.
[54] Walhout M, Megens H J L, Witte A and Rolston S L 1993 *Phys. Rev. A* **48**(2) R879–R882 https://link.aps.org/doi/10.1103/PhysRevA.48.R879
[55] Gibble K E, Kasapi S and Chu S 1992 *Opt. Lett.* **17** 526–528 https://opg.optica.org/ol/abstract.cfm?URI=ol-17-7-526
[56] Loftus T H, Ido T, Ludlow A D, Boyd M M and Ye J 2004 *Phys. Rev. Lett.* **93**(7) 073003 https://link.aps.org/doi/10.1103/PhysRevLett.93.073003
[57] Hansen D and Hemmerich A 2006 *Phys. Rev. Lett.* **96**(7) 073003 https://link.aps.org/doi/10.1103/PhysRevLett.96.073003
[58] Traverso A, Chakraborty R, Martinez de Escobar Y N, Mickelson P G, Nagel S B, Yan M and Killian T C 2009 *Phys. Rev. A* **79**(6) 060702 https://link.aps.org/doi/10.1103/PhysRevA.79.060702
[59] Kelly J F, Harris M and Gallagher A 1988 *Phys. Rev. A* **38**(3) 1225–1229 https://link.aps.org/doi/10.1103/PhysRevA.38.1225
[60] Walker T, Sesko D and Wieman C 1990 *Phys. Rev. Lett.* **64**(4) 408–411 https://link.aps.org/doi/10.1103/PhysRevLett.64.408
[61] Schussheim D and Gibble K 2018 Laser system to laser-cool and trap cadmium: towards a cadmium optical lattice clock *Frontiers in Optics / Laser Science* (Optical Society of America) p LTh1F.2 http://www.osapublishing.org/abstract.cfm?URI=LS-2018-LTh1F.2
[62] Schussheim D T and Gibble K 2023 *Review of Scientific Instruments* **94** 085101 ISSN 0034-6748 https://doi.org/10.1063/5.0157330
[63] Manzoor S, Tinsley J N, Bandarupally S, Chiarotti M and Poli N 2022 *Opt. Lett.* **47** 2582–2585 https:

//opg.optica.org/ol/abstract.cfm?URI=ol-47-10-2582
[64] Tiemann E 2022 Private Communication
[65] Bodermann B, Knöckel H and Tiemann E 2002 *The European Physical Journal D* **19** 31–44 https://doi.org/10.1140/epjd/e20020052
[66] Burns K and Adams K B 1956 *J. Opt. Soc. Am.* **46** 94–99. From their measured wavelength, it is likely that their calculated 5s5d ^{3}D$_3$ energy was 59 515.990 cm^{-1} [67]. https://opg.optica.org/abstract.cfm?URI=josa-46-2-94
[67] Kramida A 2022 Private Communication
[68] Büki M, Röser D and Stellmer S 2021 *Appl. Opt.* **60** 9915–9918 https://opg.optica.org/ao/abstract.cfm?URI=ao-60-31-9915